Food Hydrocolloids 67 (2017) 120–129

Contents lists available at ScienceDirect

Food Hydrocolloids

journal homepage: www.elsevier.com/locate/foodhyd

Submicron O/W emulsions embedded into modified waxy maize starch based matrix: Rheological and microstructural characterization

E.H. Alfano [a], T. Crosta [a], M.J. Martinez [b, c], O.E. Pérez [d], M.E. Farías [a, b, e, *]

[a] Universidad Nacional de Luján, Departamento de Tecnología, Ruta 5 y 7, Luján, 6700, Buenos Aires, Argentina
[b] Universidad de Buenos Aires, Departamento de Industrias, Facultad de Ciencias Exactas y Naturales, Intendente Güiraldes, s/n, Ciudad Universitaria, Buenos Aires, 1428, Argentina
[c] ITAPROQ-CONICET, Universidad de Buenos Aires, Facultad de Ciencias Exactas y Naturales, Intendente Güiraldes, s/n, Ciudad Universitaria, Buenos Aires, 1428, Argentina
[d] IQUIBICEN-CONICET, Universidad de Buenos Aires, Departamento de Química Biológica, Facultad de Ciencias Exactas y Naturales, Intendente Güiraldes, s/n, Ciudad Universitaria, Buenos Aires, 1428, Argentina
[e] CIC, Comisión de Investigaciones Científicas de la Provincia de Buenos Aires, Argentina

ARTICLE INFO

Article history:
Received 8 September 2016
Received in revised form
22 December 2016
Accepted 28 December 2016
Available online 3 January 2017

Keywords:
Submicron emulsions
Modified starch
Mixed colloidal suspension
Steady flow
Frequency sweep

ABSTRACT

The aim of this study was to investigate the rheological properties and storage stability of submicron O/W emulsions formulated with dried skim milk and vegetable oil at neutral pH, and to analyse the impact of their inclusion into starch suspension. Sunflower oil droplets were pre-emulsified in skim milk suspension by a rotor-stator homogenizer and further an ultrasonic treatment was applied. Droplets sizes decreased after applying ultrasound (US) from 1.4 to 0.4 μm (d_{32}). Emulsions exhibited Bingham flow behaviour and the plastic viscosity increased upon 14 days of storage at 5 °C. Flocculation may be responsible for the increase in viscosity with aging time. Mixed colloidal dispersions (submicron emulsions embedded into starch matrix) showed shear-thinning behaviour. Over storage, light microscope micrographs suggested deposited droplets on the starch granules surface. Flow and viscoelastic behaviour of mixed colloidal dispersions indicated droplets flocculation, attributable to a reversible depletion mechanism of destabilization.

1. Introduction

Foods are complex multiphasic systems containing mixtures of diverse kinds of particles, for example, a mixture of large starch granules and small oil droplets, which is considered by the literature as model systems of semi-solid food products, like many sauces, desserts, and dressings (Chung, Degner, & McClements, 2012). Typically, the droplet size of conventional food emulsions is larger than 1 μm, but submicron emulsions can be defined as a class of emulsions with a droplet size between 20 and 500 nm (Camino & Pilosof, 2011). Potential advantages of submicron emulsions over conventional emulsions such as high physical stability against sedimentation and creaming and low turbidity make them attractive systems for application in food industry (Camino & Pilosof, 2011; Ghosh, Mukherjee, & Chandrasekaran, 2013). Preparation of these emulsions involves high energy input and it can be done for instance using an ultrasound (US) homogenizer device. The application of US in the food industry is interesting for quality and safety improvement of processed foods (Chandrapala, Martin, Kentish, & Ashokkumar, 2014). The physical effects of high intensity US (mechanical vibration, microstreaming and intense shear forces) generated by acoustic cavitation are considered to be the main reason for the generation of emulsions (Shanmugam & Ashokkumar, 2014a). At this respect, these authors reported the incorporation of 7% of flax seed oil in pasteurized homogenized skim milk (3.3% total protein) using just US without milk fat globular membrane and other food additives. Flow properties of these emulsions resulted stable at least 9 days at 4 ± 2 °C.

In the present work, the selection of skim milk powder is based on the fact that it is a crucial ingredient incorporated to a variety of products such as sauces and deserts, besides the high biological values of its proteins. Also, milk protein functionality during drying, storage and further reconstitution in water is retained (Chandrapala et al., 2014). On the other hand, casein-whey

* Corresponding author. Universidad Nacional de Luján, Departamento de Tecnología, Ruta 5 y 7, Luján, 6700, Buenos Aires, Argentina.
E-mail address: efarias@mail.unlu.edu.ar (M.E. Farías).

http://dx.doi.org/10.1016/j.foodhyd.2016.12.038
0268-005X/

aggregates present in skim milk powder were disrupted by exposure to ultrasound being their physicochemical properties unaffected (Chandrapala, Martin, Zisu, Kentish, & Ashokkumar, 2012).

Modified waxy maize starch is composed mainly of highly branched amorphous amylopectin and it used as thickener in emulsified systems like soups, bakery fruit filling, sauces, salad dressing (Bortnowska, Balejko, Tokarczyk, Romanowska-Osuch, & Krzemińska, 2014). Modified waxy maize starch dispersions can be considered as swollen gelled particles dispersed in a phase constituted only by water (Nayouf, Loisel, & Doublier, 2003). There is scarce information about submicron emulsions formed by US whose drops have been included into a modified waxy maize starch based matrix. Starch is common ingredient on food suspension or emulsions added during their preparation and processing. Size of colloidal particles in food products has a substantial impact on the product characteristics, for instance physicochemical, functional and sensory properties (Aernouts et al., 2015). The objective of this contribution was to characterize O/W submicron emulsions prepared with skim milk proteins as emulsifier and to analyse the impact of their incorporation into a modified waxy maize starch based matrix. The rheological parameters, droplets size distribution and microstructure of these complex systems were determined as well as their evolution upon storage time.

2. Materials and methods

2.1. Materials

Commercial skim milk powder was provided by Nestlé (Argentina). Milk powder composition was: 50 wt% carbohydrates (mainly lactose), 35 wt% protein and 0 wt% lipid; as detailed by the manufacturer. Polartex™ 06730 modified starch (kindly supplied by Cargill, Argentina) was a stabilized and crosslinked waxy maize starch. Milk suspension was previously hydrated at 5 °C for 24 h. Commercial high oleic sunflower oil was provided by Molino Cañuelas SACIFIA (Cañuelas, Argentina). Milli-Q ultrapure water was used as the solvent. The pH of starch suspension, emulsions and mixed colloidal systems ranged 6.5–7.0.

2.2. Emulsions preparation

The emulsions compositions were:

E1: 74 g water, 15 g skim milk powder, 1 g sodium azide solution (1 wt%) and 10 g oil
E2: 64 g water, 15 g skim milk powder, 1 g sodium azide solution (1 wt%) and 20 g oil.

Firstly, aqueous phase was prepared in a glass vessel by dissolving the proper amount of powdered skim milk into water. Secondly, 100 g pre-emulsions were created by mixing both phases together using an Ultra-Turrax® model T2 Basic rotor-stator homogenizer (IKA-Labortechnik, Staufeni, Germany), operating at 10,000 rpm for 2 min. Container volume was 250 ml. The complete homogenization was achieved by sonication with a concomitantly submicron emulsion formation. To this end, 7 mL of each pre-emulsion were treated with an Omni Ruptor 4000 sonicator provided by a titanium microtip of diameter 3.8 mm (OMNI International Inc., Kennesaw, GA, USA). The microtip was immersed into the emulsion at a depth of 10 mm to prevent foam formation. The sonication process was performed for 2 min at 40% power (400 W) of 20 kHz. To prevent excessive heating, the samples were immediately placed in ice and water baths. Emulsions were stored at 5 °C.

2.3. Starch suspension

Starch suspension was obtained by dissolving the corresponding amount of waxy modified starch (S) in distilled water, to give final concentrations of 4 wt%, for no oil phase added systems, and 5 wt%, for experimental controls with oil phase. Glass beaker containing starch suspensions were put on a hot plate. The suspension boson temperature was kept at 90 °C for 6 min under stirring to finally being cooled at room temperature.

2.4. Starch and milk protein mixed dispersion

7 mL of skim milk suspension (15 wt%) was sonicated as described in Section 2.2. Dispersion were prepared by mixing 1 g of sonicated skim milk suspension and 4 g of starch suspension (5 wt %) in a magnetic stirrer. The final mixture (USMS) composition was 4 wt% starch and 3 wt% skim milk. In order to comparison, a mixture (MS) was prepared with no sonicated skim milk.

2.5. Mixed colloidal dispersion: starch matrix inclusion

For convenience, mixed colloidal dispersions were prepared by mixing 1 g of US emulsion (E1 or E2) and 4 g of starch suspension (5 wt%) under magnetic stirring.

The final mixtures compositions were:

SE1: starch (4 wt%), skim milk powder (3 wt%) and oil (2 wt%)
SE2: starch (4 wt%), skim milk powder (3 wt%), and oil (4 wt%).

Starch suspensions and mixed colloidal dispersions were stored at 5 °C.

2.6. Microscopy observation

The microstructure was examined using optical microscopy with a 40× objective lens and 10× eyepiece (Carl Zeiss, German) equipped with a digital camera (Q-Color 3C, Canada). A small drop of emulsions was situated on the microscope slide and covered with a coverslip prior to analysis. 10 μl of Lugol reagent was added at mixed colloidal dispersion under analysis. Several micrographs were obtained per sample at days 0, 7 and 14.

2.7. Particle size measurements

Particle size of starch granules and oil droplet size of emulsions were determined by static light scattering using a Mastersizer 2000 with a Hydro 2000MU unit (Malvern Instruments, Malvern, UK). Measurements were performed for starch suspensions in water (obscuration in the range of 10–15%), at the rate of pump of 1800 rpm. A refractive index of 1.33 was used for the aqueous phase, 1.43 for the oil phase in emulsions and 1.50 for the starch phase in starch suspensions and mixed colloidal dispersions, conditions used by Chung et al. (2012). Particle and droplet sizes were informed as the volume-surface mean diameter or Sauter diameter ($d_{3,2} = \sum n_i d_i^3 / \sum n_i d_i^2$) and the equivalent volume-mean diameter or De Broucker diameter ($d_{4,3} = \sum n_i d_i^4 / \sum n_i d_i^3$) where n_i is the number of particles of diameter d_i (Camino & Pilosof, 2011). Emulsions are usually greatly polydisperse, with droplet radii certainly spanning (Robins, Watson, & Wilde, 2002). Span (polydispersity) was calculated with the formula: Span $= (d_{0.9}\text{-}d_{0.1})/d_{0.5}$ where, $d_{0.9}$, $d_{0.1}$, and $d_{0.5}$ are the diameters at 90%, 10%, and 50% of cumulative volume, respectively (Turasan, Sahin, & Sumnu, 2015). The surface area per mass unit of the dispersed phase (SSA) was obtained by the analysis of results generated by measurements.

2.8. Rheological characterization

The rheological properties of systems were carried out with a rheometer (Physica MCR 301, Anton Paar, Germany) equipped with a cone and a plate geometry sensor (50 mm diameter, 1° cone angle and 0.099 mm gap) and a Peltier temperature controlling system. 560 μL of samples was placed in the determination platform of the instrument. Measurements were made at day 0, 7 and 14.

2.8.1. Steady flow

Steady flow tests of all systems was measured at 25 °C using shear rates from 0 to 300 s^{-1} at 25 °C to obtain shear rate versus shear stress data according to Guo et al. (2015). The experimental data of suspensions were fitted to the Power Law's model (equation (1)):

$$\tau = K\dot{\gamma}^n \quad (1)$$

where τ is the shear stress (Pa), $\dot{\gamma}$ is the shear rate (s^{-1}), K is the consistency coefficient (Pa.s^n), which is commonly homologated with the viscosity and n (dimensionless) is the flow behaviour index. Samples with a power low index (n) close to unit were also analysed using Bingham's rheological model (Tadros, 2004), $\tau = \tau_0 + \eta\dot{\gamma}$, where the slope is the plastic viscosity (η) and the intercept is the yield stress (τ_0).

2.8.2. Dynamic shear measurement

Dynamic frequency sweeps were performed over an angular frequency (ω) range of 100 to 0.1 rad s^{-1} by applying a constant strain (0.5%) which was within the region of linear viscoelasticity at 25 °C. Storage modulus (G'), loss modulus (G'') and loss tangent angle ($\tan\delta = G''/G'$) were obtained as a function of $f = \omega/2\pi$.

2.9. Visual observation of phase separation

Phase separation of emulsions and mixed colloidal dispersions after storage was determined visually during 14 days by measuring the height of gravitational oil phase separation in O/W emulsion, transferring 5 mL of each emulsion into a graduated tube immediately after emulsion preparation (Abdolmaleki, Mohammadifar, Mohammadi, Fadavi, & Meybodi, 2016). Samples were sealed with Parafilm® films to prevent evaporation and stored at 5 °C.

2.10. Statistical analysis

Each sample was investigated at last in duplicate from independently prepared samples. Data were subjected to ANOVA analysis applying the Tukey's test at $p < 0.05$ using the GraphPad Prims v6.0 (GraphPad Software, San Diego, CA, USA).

3. Results and discussion

3.1. US emulsions characterization

The particle size distributions of non-sonicated E1 and E2 emulsions were bimodal and resulted in larger volume of droplets ranging from 0.1 to 25 μm (Fig. 1A and B). Table 1 shows $d_{3,2}$ and $d_{4,3}$ indexes, span values and the specific surface area (SSA) values of non-sonicated E1 and E2. As can be seen from Table 1, $d_{3,2}$ indexes were 1.2 and 1.3 μm and the $d_{4,3}$ indexes were 6.7 μm and 6.1 μm of non-sonicated E1 and E2, respectively. The $d_{4,3}$ index is affected by large particles, whereas the $d_{3,2}$ is influenced by the smaller ones (Bortnowska et al., 2014). The polydispersity index, as analysed by span values, of the non-sonicated E1 and E2 emulsions ranged between 2.4 and 2.9 (Table 1).

Table 1
Mean diameter ($d_{3,2}$ and $d_{4,3}$), span and specific surface area (SSA) of emulsions.

	$d_{3,2}$ (μm)*	$d_{4,3}$ (μm)*	Span*	SSA (m^2/g)*
Not sonicated E1$^+$	1.19 ± 0.03^b	6.69 ± 0.04^a	2.91 ± 0.03^a	5.03 ± 0.13^a
Not sonicated E2$^+$	1.32 ± 0.03^a	6.09 ± 0.02^b	2.35 ± 0.01^b	4.52 ± 0.08^b
E1$^△$	0.42 ± 0.01^B	0.73 ± 0.01^B	2.62 ± 0.06^A	14.33 ± 0.37^A
E2$^△$	0.48 ± 0.01^A	0.79 ± 0.01^A	2.28 ± 0.03^B	12.62 ± 0.10^B

*Mean ± SD corresponding to ten measurements made on two independently prepared samples.
$^{+△}$Means with the same letter in the same column are not significantly different at $p < 0.05$.

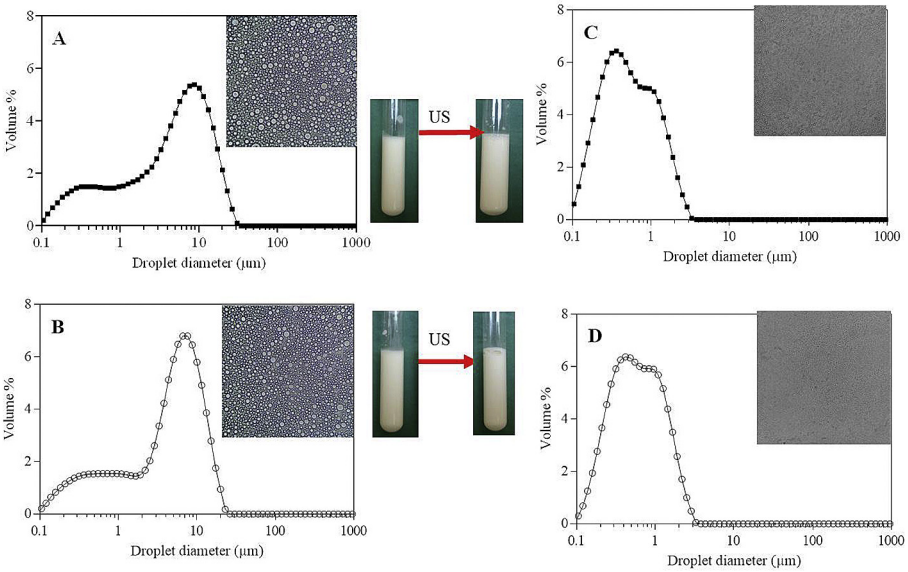

Fig. 1. Volume droplet size distributions and microstructure (inserts, magnification: 400×) corresponding to E1 (A) and E2 (B) emulsions by homogenization and E1 (C) and E2 (D) by homogenization + US (t = 0). Macroscopic appearances of emulsions are included. Each point of droplet size distribution corresponds to the mean of ten readings made on two independently prepared emulsions.

A decrease in droplet size distributions of emulsions could be observed after applying US, Fig. 1C and D, which was visualized as a tendency towards unimodal size distribution in a range between 0.1 μm and 3 μm. Table 1 clearly showed that US had a significant effect on decreasing the droplet size. The specific surface areas (SSA) calculated using the diameter $d_{3,2}$, resulted three times higher for US emulsions (E1 and E2). Canselier et al. (2002) have described US emulsification as a two-step process: in the first step, the turbulence caused by the mechanical vibration leads to the eruption of dispersed phase droplets into the continuous phase and the second step consists of droplets breaking up through the shear forces generated by cavitation at the interface. The $d_{4,3}$ and $d_{3,2}$ indexes ranged between 0.7-0.8 μm and 0.4–0.5 μm, respectively (Table 1). The emulsion stability is closely associated to the droplet size

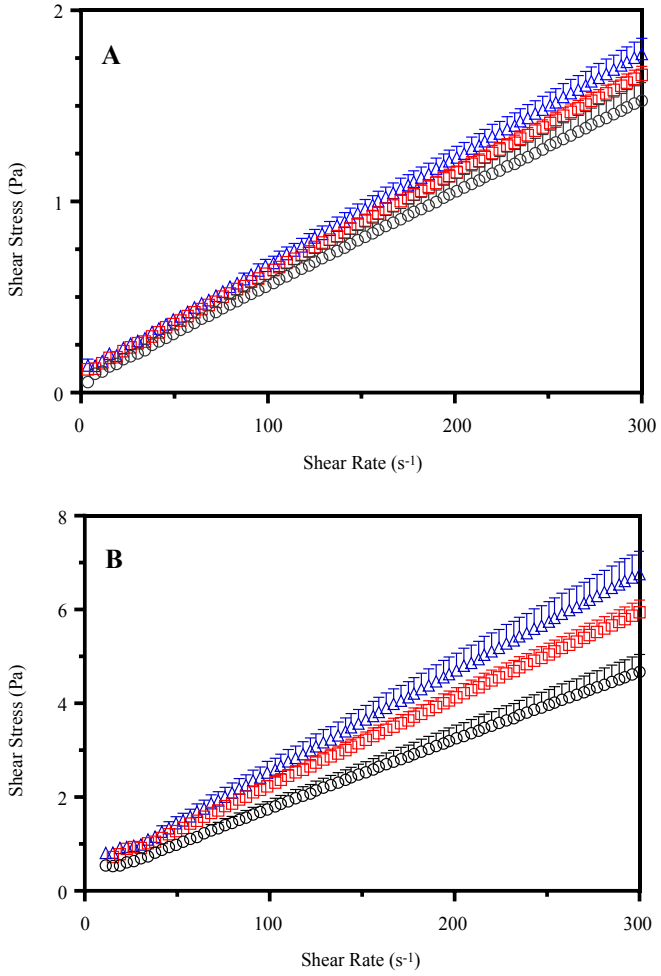

Fig. 2. Flow curves for US (A) E1 and (B) E2 emulsions during the storage time (days): 0 (◯); 7 (□) and 14 (△). Bars represent standard error of the mean (n = 4).

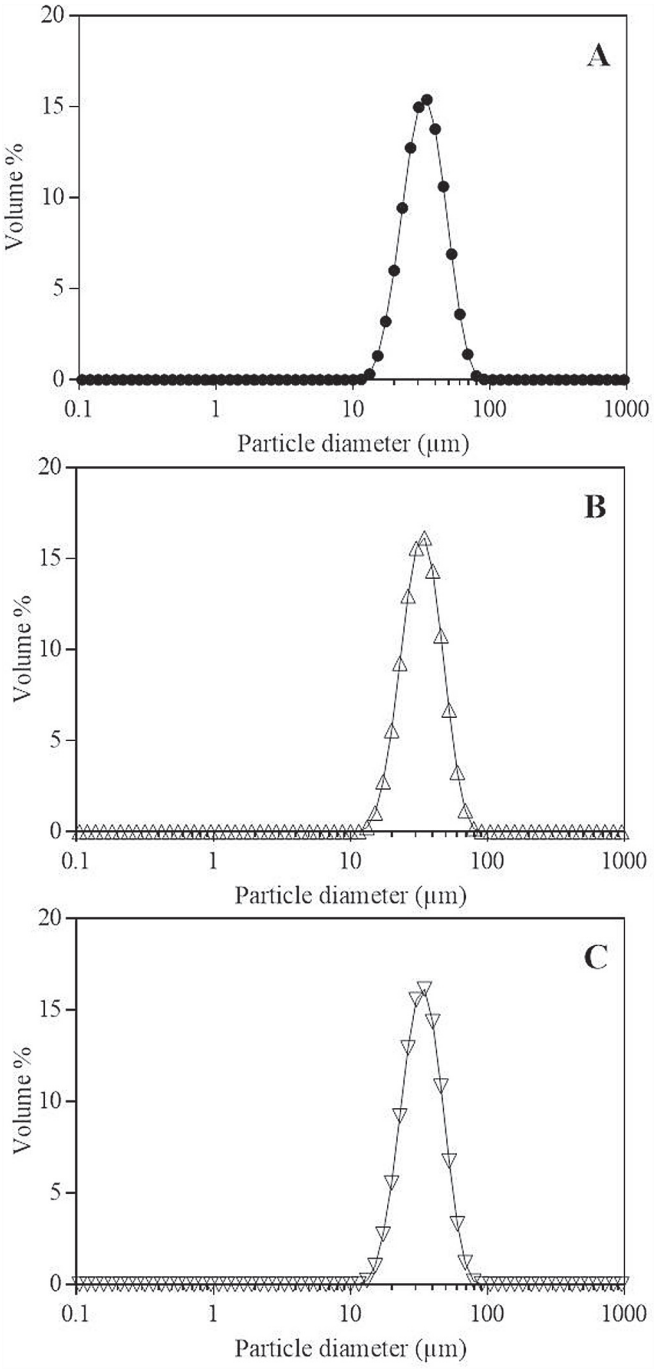

Fig. 3. Volume particle size distributions of S (A); SE1 (B) and SE2 (C). Each point corresponds to the mean of ten readings made on two independently prepared samples. Starch suspension (S). Mixed colloidal systems: SE1 (starch suspension - US E1 emulsion) and SE2 (starch suspension – US E2 emulsion).

Table 2
Parameters derived from the Bingham's model application on flow curves corresponding to US E1 and E2 emulsions.

Time (days)	E1			E2		
	η (mPa.s)	τo (Pa)	R^2	η (mPa.s)	τo (Pa)	R^2
0	4.90 ± 0.01[a]	0.066 ± 0.001[a]	0.9998	14.78 ± 0.05[a]	0.38 ± 0.01[a]	0.9992
7	5.20 ± 0.01[b]	0.100 ± 0.001[b]	0.9999	18.65 ± 0.07[b]	0.46 ± 0.01[b]	0.9991
14	5.60 ± 0.01[c]	0.110 ± 0.001[b]	0.9999	21.36 ± 0.07[c]	0.55 ± 0.01[c]	0.9991

Average ± standard error (n = 4) are informed.
Means with the same letter in the same column are not significantly different at $p < 0.05$.

Table 3
Mean diameter ± standard deviation ($d_{3,2}$ and $d_{4,3}$), span and specific surface area (SSA) of samples.

	$d_{3,2}$ (μm)	$d_{4,3}$ (μm)	span	SSA (m^2/g)
S	33.14 ± 0.04^A	37.13 ± 0.04^A	0.90 ± 0.01^A	0.181 ± 0.005^A
SE1	33.47 ± 0.04^B	37.18 ± 0.04^B	0.86 ± 0.01^B	0.200 ± 0.005^B
SE2	33.51 ± 0.04^B	37.24 ± 0.04^C	0.86 ± 0.01^B	0.200 ± 0.005^B

Mean ± standard deviation corresponding to ten measurements made on two independently prepared samples.
Means with the same letter in the same column are not significantly different at $p < 0.05$.

distribution. The distribution patterns of US E1 and US E2 were similar; this fact assumes that the skim milk powder concentration was enough to equally minimize the droplet size in both formulations.

Sonication energy is not enough to generate stable emulsions by its own, being milk proteins the most important factor for emulsion droplets stabilization. Milk proteins are mainly, a complex and heterogeneous mixture of caseins (αs1-, αs2, β-, and κ-) and β-lactoglobulin which are known that rapidly adsorb at the oil-water interface conferring a low interfacial tension during emulsification; also, the two major individual caseins, (αs1- and β-), are knowing as extremely effective emulsifying agents (Bouyer, Mekhloufi, Rosilio, Grossiord, & Agnely, 2012). Arzeni et al. (2012) studied comparatively the impact of high intensity ultrasound (HIUS) on the functionality of some of the most used food proteins at the industrial level: whey protein concentrate (WPC), soy protein isolate and egg white protein. These results obtained suggest that the HIUS treatment induced a certain degree of molecular unfolding of the protein molecules causing more hydrophobic groups and regions inside the molecules to be exposed to the more polar surrounding

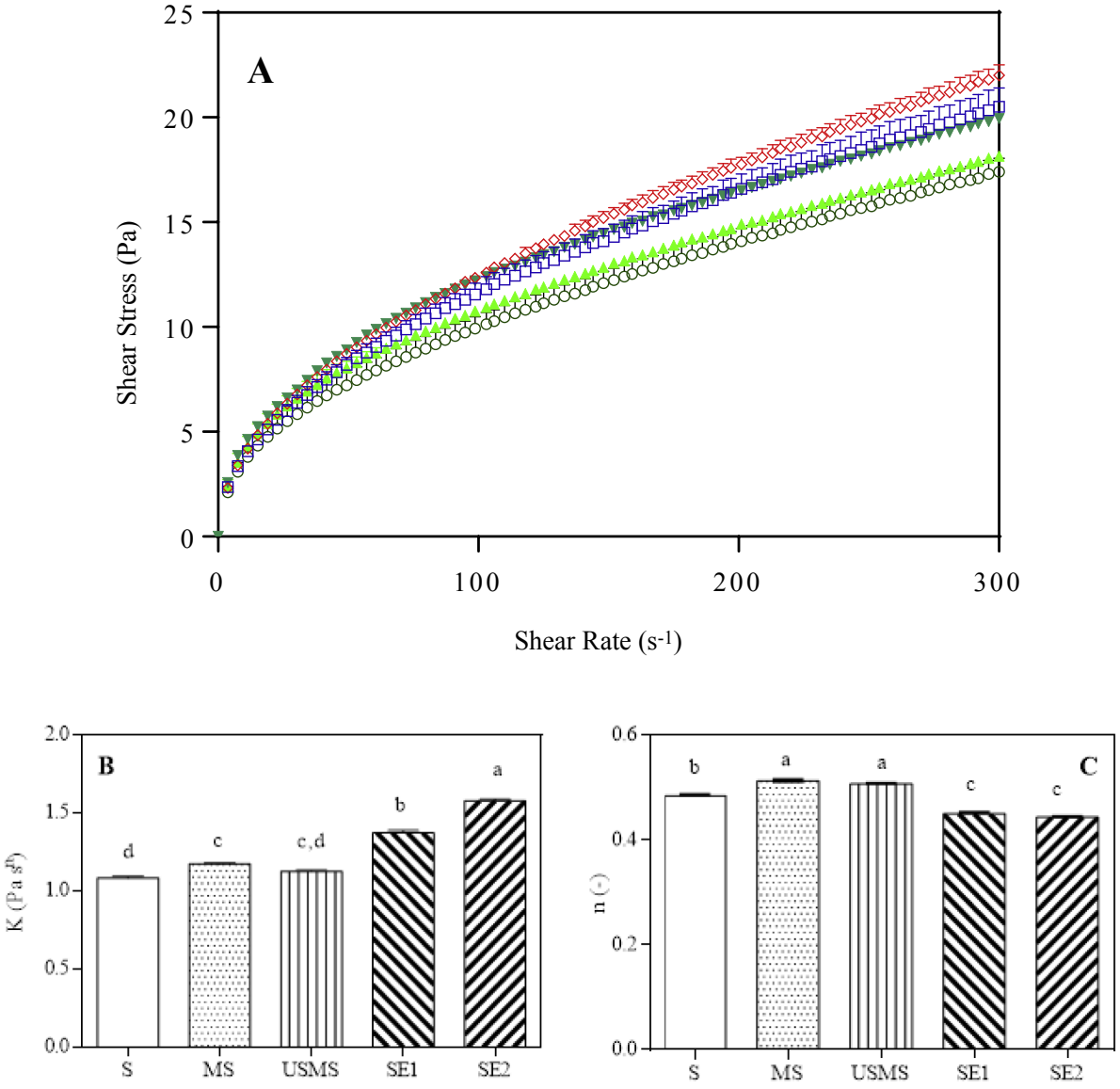

Fig. 4. (A) Flow curves for S (◯); MS (◇); USMS (□); SE1 (▲) and SE2 (▼) systems at initial time (day = 0). The means values are represented (n = 4). Bars represent standard error of the mean. (B) *K* and (C) *n* values obtained by the Power Law model for S, MS, USMS, SE1 and SE2. $R^2 > 0.997$. Means with a different letter are significantly different ($p < 0.05$). Bars represent standard error of the mean. Starch suspension (S). Mixed colloidal systems: MS (starch suspension − skim milk); USMS (starch suspension − US skim milk); SE1 (starch suspension - US E1 emulsion) and SE2 (starch suspension − US E2 emulsion).

environment. On the other hand, de Figueiredo Furtado, Mantovani, Consoli, Hubinger, and da Cunha (2017) working with sodium caseinate and lactoferrin found similar results. Therefore, the hydrophobicity increase upon US application seems to be a general effect more than a specific one. Thus, the hydrophobicity of the proteins enhancing their adsorption at the oil-water interface improved their emulsifier capacity (Arzeni et al., 2012; O'Sullivan, Murray, Flynn, & Norton, 2016; Shanmugam & Ashokkumar, 2014b). It is important to say that the emulsifying capacity of the proteins do not depend only on their hydrophobicity. The ultrasound can modify other properties that affect the capacity of emulsification of the proteins such as their size and electric charge i.e. the ultrasound treatment reduces the size of protein (Arzeni et al., 2012). As is well known, the rate of adsorption depends on the molecular size and shape and the chemical nature of the protein surface, such as the hydrophobicity, among other factors.

The microstructures of non-sonicated and US emulsions are inserted in each plot in Fig. 1. They clearly demonstrate the effect of ultrasonic homogenization on the size of oil droplets, which were so small to be detectable with an optical microscope. However, the non-sonicated and US emulsions were visually similar in terms of appearance to milk.

Physical stability during storage time is an important property of dispersed systems, i.e. emulsions and foams. US emulsions could be stored until 14 days, with indistinguishable phase separation or creaming. In contrast, non-sonicated emulsions showed important creaming separation after 7 days, 24% and 37% for E1 and E2 respectively (not shown).

The flow properties of US emulsions are showed in Fig. 2A and B. It can be see that the shear stress increased linearly as the shear rate increased. The η of both US emulsion, E1 and E2, was 4.9 mPa s and 14.8 mPa s, respectively, at immediately sonication treatment was applying (t = 0) (Table 2). The yield values, τ_0, obtained by extrapolation of the shear stress-shear rate curve to zero (Tadros, 2004) were 0.07 Pa and 0.38 Pa, respectively. The US E1 emulsion tended to that Newtonian fluid because their viscosity values were in practice equal to the plastic viscosity, η. Newtonian flow behaviour is quite common in US emulsions. For example, Bellalta, Troncoso, Zúñiga, and Aguilera (2012) found that O/W emulsions stabilized by whey protein isolate containing 50 and 55% oil proportion exhibited a Newtonian flow behaviour. The greatest oil fraction US emulsion (E2) shifted the flow curves to higher plastic viscosity, which could be attributed to the increased packing of the oil droplets (Kaltsa, Spiliopoulou, Yanniotis, & Mandala, 2016).

The stability studies of US emulsions upon time were analysed based on rheological measurements. Measurements were carried out at 7 and 14 days after emulsion preparation (Fig. 2 and Table 2). US application showed their effect on rheological parameters of emulsions during the storage time; even though the Bingham behaviour was not altered. The greatest changes were notice for 20 wt% oil emulsion (E2). Thus, during the 14 days of storage, η and τ_0 increased 14% and 67% respectively for E1 and 40 and 45%, for E2. Viscosity values increase may be related to destabilization processes operating between emulsion droplets, being the flocculation the predominant one when the droplet size distribution remains constant (Sosa, Schebor, & Pérez, 2014; Tadros, 2004). According to Tadros (2004), the Ostwald ripening and/or coalescence result in a shift of the droplet size distribution to higher diameters; this effect also reduces the viscosity and τ_0. If flocculation occurs simultaneously the net effect may be an increase or decrease of the rheological parameters. It was important to say that flocculation, sedimentation and creaming are reversible mechanisms of droplets migration, whereas Ostwald ripening and coalescence are not. These results pointed out that the negatively charged adsorbed protein molecules (casein pI 4.6) on the surfaces of oil droplets prevented the destabilization of emulsion possibly via electrostatic repulsion. This phenomenon is favoured at neutral pH due to the presence of covered protein surfaces on these emulsion droplets (Shanmugam & Ashokkumar, 2014a).

In summary, the mechanical vibration and acoustic cavitation of US are responsible for the mixing of the two immiscible phases, oil and aqueous, and the increased emulsifier properties generated on milk proteins. The consequence is the formation of stable emulsions where the flocculation would be the predominant mechanism of destabilization. Flocculation could be attributed to unabsorbed milk aggregates (protein and carbohydrates) from the bulk aqueous phase (Dickinson, Golding, & Povey, 1997).

3.2. Starch suspension characterization

Firstly, in this part of the study, the modified waxy starch suspension, S, was characterized in order to use it as a component of the continuous phase. Fig. 3A shows a monomodal volume size distribution of S (4 wt%). The $d_{3,2}$ and $d_{4,3}$ indexes derived from particle size distribution were 33 μm and 37 μm, respectively (Table 3), these latest values were coincident to that found for heating waxy modified corn starch granules (Chung et al., 2012; 2014).

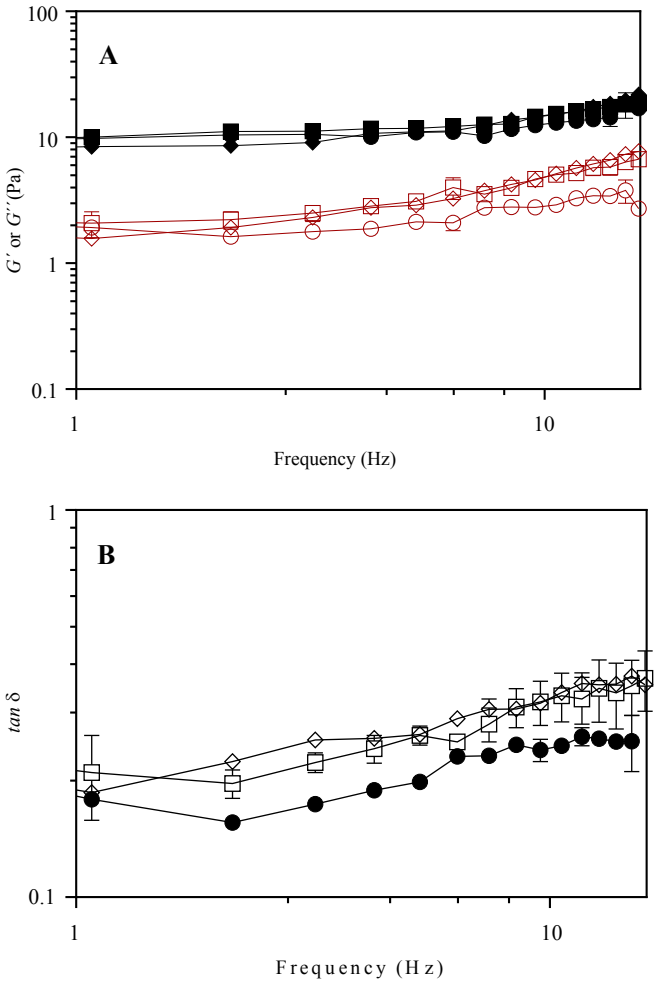

Fig. 5. A) Mechanical spectra for S (●, ○); MS (◆, ◇) and USMS (■, □), at 25 °C. Solid and empty symbols represent G' and G'', respectively. Bars represent standard error of the mean (n = 3). B) *Tan δ* of S (●); MS (◇) and USMS (□).Starch suspension (S). Mixed colloidal systems: MS (starch suspension − skim milk) and USMS (starch suspension − US skim milk).

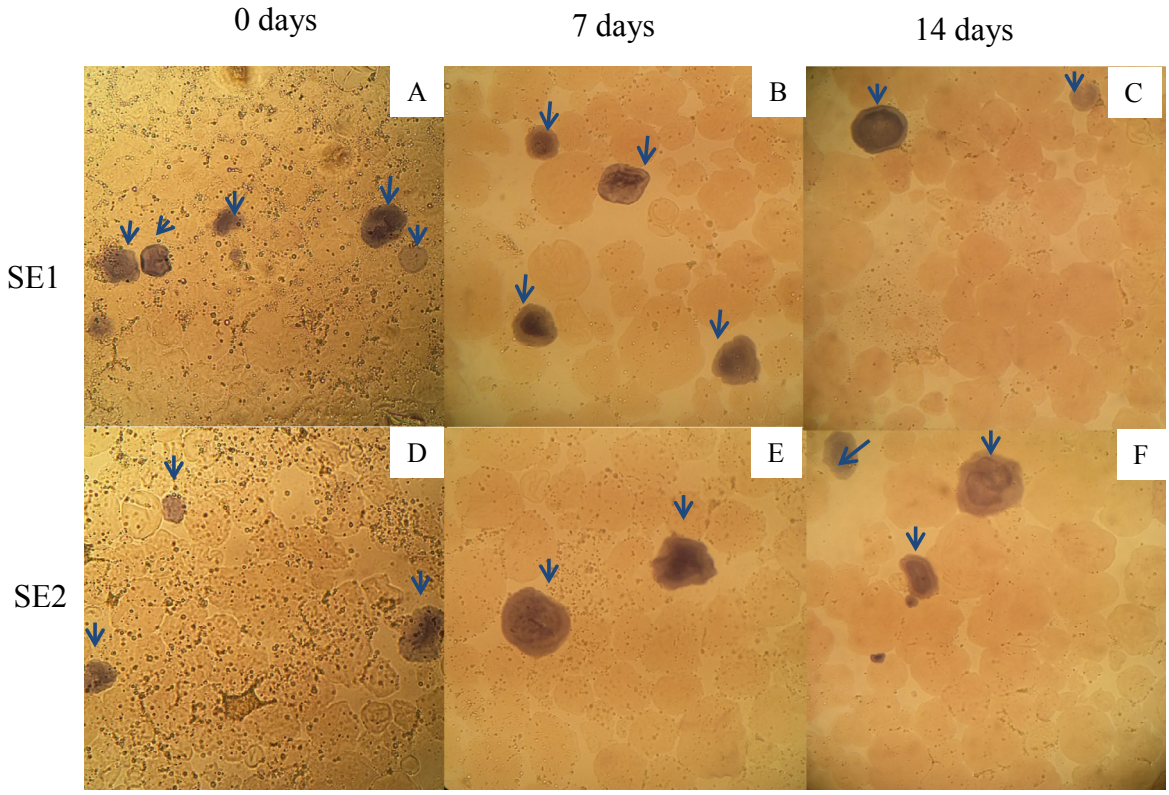

Fig. 6. Microstructure corresponding to SE1 (A, B and C) and SE2 (D, E and F) mixed colloidal suspension during the storage time (days): 0 (A y D), 7 (B and E) and 14 (C and F). All micrographs are of the same scales and magnification, 400×. Blue-stained starch granules are identified with blue arrows. Mixed colloidal systems: SE1 (starch suspension - US E1 emulsion) and SE2 (starch suspension − US E2 emulsion). (For interpretation of the references to color in this figure legend, the reader is referred to the web version of this article.)

The steady flow behaviour of S is shown in Fig. 4A. The increase in flow rate with shear stress of S was non-linear, indicative of shear thinning behaviour, and it was fitted by the Power Law's model (R^2 = 0.9992). *K* and *n* were 1.083 ± 0.021 and 0.485 ± 0.002, respectively (Fig. 4B and C). Gelatinized modified starch dispersion can be described as just a suspension of swollen particles, in which the flow behaviour are mostly governed by the volume fraction and the deformability of swollen starch granules, depending on concentration (Morell, Fiszman, Varela, & Hernando, 2014).

Skim milk incorporation into starch suspension (MS) slightly increased *K* index (1.173 ± 0.009) and *n* index (0.513 ± 0.001) (Fig. 4B and C), which is attributable to the higher viscosity of the dispersing phase, due to the presence of milk proteins (Tárrega, Vélez-Ruiz, & Costell, 2005).

Mechanical spectra (*G′* and *G″* as a function of frequency) for S, MS and USMS suspensions are illustrated in Fig. 5A. All starch suspensions, exhibited a solid like behaviour being $G' > G''$ and *G″* modulus showed ascending tendency with increasing frequency. Tan *δ* compares the amount of energy lost to the amount of energy stored indicating the elastic or viscous properties predominance (Bortnowska et al., 2014). It was noticed that in S, MS and USMS samples, the tan *δ* values were lower than 1, however greater than 0.1 indicating weak gels (Fig. 5B). The tan *δ* curves revealed ascending tendency throughout the tested frequency range, showing the variations in interactive forces maintaining the gel network (Bortnowska et al., 2014). This behaviour was characteristic for cross-linked starch suspensions which was attributed to close-packing of swollen starch granules (Vu Dang, Loisel, Desrumaux, & Doublier, 2009). It also can be noticed in the same Fig. 5A and B that the viscoelastic behaviour of MS and USMS was similar. These overall tendencies indicated that the factor governing the viscoelastic and flow behaviour of these suspensions was structured by the packing of the swollen starch granules (Nayouf et al., 2003).

3.3. Characterization of systems formed with submicronic emulsions included into waxy starch based matrix

In the case of US emulsions, the fat droplets size distributions gave a broad peak at a diameter between 0.1 and 3 μm (Fig. 1C and D), whereas the starch granules in the starch suspension gave a peak between 10 and 100 μm (Fig. 3 A). It can be notice in Fig. 3B and C and Table 3 that the particle size distributions for mixed colloidal dispersions were monomodal with a large peak around 30 μm which practically coincided with the particle size of starch suspension. Here, it is worth to highlight the findings of Chung et al. (2012), who have noted the absence of the smaller peak (corresponding at oil droplets) in complex systems (5 wt% starch), containing ≤ 10% oil proportion. Authors attributed this fact to different refractive indices for starch granules and oil droplets; therefore starch granules scatter light more strongly, being the instrument more sensitive to larger particles than smaller ones.

Flow curves of mixed colloidal dispersions (SE1 and SE2) were showed in Fig. 4A. All samples exhibited shear thinning behaviour, indicating that the starch granules played a principal role in determining the overall rheology of the mixed colloidal dispersions. It can pointed out that the systems with 4 wt% oil droplets (SE2) had higher apparent viscosities than 2 wt% (SE1) ones which may be a result of a lubrication effect associated with the oil droplets (Wu & McClements, 2015). Experimental flow data were well fitted with the Power Law model obtaining high correlation coefficient R^2 between 0.998 and 0.999. Constants derived from the

model were showed in Fig. 4B and C. *K* increased and *n* decreased in SE emulsions in comparison to starch suspensions, indicating the intensification of shear-thinning behaviour. Tárrega et al. (2005) studied the influence of the addition of whole milk on the pasting, flow and viscoelasticity behaviours of dispersions of three cross-linking modified starches. They found that the apparent viscosity was higher in starch-milk (3.12 wt% fat) than in starch-water suspension, concluding that some milk components, like casein or fat, increase the starch granules rigidity.

The microstructure of emulsion included into a starch based matrix is shown in Fig. 6. It could be appreciated swollen starch granules, which were brown stained and some individual blue-stained granules, corresponding to starch granules with a higher amylose content (Morell et al., 2014). The finely emulsified oil droplets previously generated by the intense shear forces of US can be seen with an optical microscope and are noticed in the surfaces of starch granule. According to the literature, the swelling of the starch granules reduces the volume of aqueous phase and therefore increases droplet interactions (Chung, Degner, & McClements, 2014). Upon 7 days of storage, oil droplets approach on the starch granules surfaces was more remarkable. Starch granules looked like more swelled due to water absorption. Droplet flocculation was evident upon 14 days of storage (Fig. 6). None of mixed colloidal dispersions upon storage showed any visible signs of physical instability (phase separation or creaming).

Upon storage, the mixed colloidal dispersions (USMS, SE1 and SE2) under the shear rate as a function of shear stress showed shear thinning behaviours which also were well described by power law with high coefficients of determinations ($R^2 > 0.965$) (Fig. 7).

As expected, the effect of storage on *K* and *n* indexes corresponding at flow behaviour of USMS was not appreciated ($p > 0.05$) (Fig. 7A).

Mixed colloidal dispersions had an unexpected opposite behaviour. An increase of *K* indexes of SE1 (from 1.372 ± 0.028 to 1.744 ± 0.111 Pa.s^n) and SE2 (from 1.577 ± 0.011 to 2.351 ± 0.084 Pa.s^n) evidenced oil droplets flocculation mechanism predominance at 7 days of storage (Fig. 7B and C). *K* indexes did not change between 7 and 14 days in both mixed colloidal dispersions. On the other hand, *n* indexes of SE1 not had changes after 14 days of storage (0.450 ± 0.040) ($p > 0.05$). However, *n* indexes of SE2 decreased from 0.444 ± 0.001 to 0.417 ± 0.007) at 7 days of storage, then remained constant. Georgiadis et al. (2011) explained that in high-shear stresses the floc structures are generally disrupted being the viscosity of systems dependent on the rheology of the continuous phase. To quantify this effect, the apparent viscosity of SE1 and SE2 were recorded at 300 s^{-1} during storage. Apparent viscosities of SE1 and SE2 were: 0.065 ± 0.007 and 0.066 ± 0.001 Pa s. Results showed that apparent viscosities at 300 s^{-1} of both systems were independent of storage time ($p > 0.05$).

Viscoelastic properties of the mixed colloidal dispersions (USMS, SE1 and SE2) upon storage were plotted as a function of the oscillation frequency in Fig. 8. The oscillation test revealed that all suspensions exhibited similar predominantly elastic-like behaviour being *G′* higher than *G″* over the range of frequencies tested. In USMS, SE1 and SE2 samples, *G″* moduli demonstrated ascending tendency with increasing frequency (Fig. 8A, B and C). Tan *δ* curves (Fig. 8D, E and F) also exhibited arising tendency throughout the tested frequency range. This shows that the studied systems had structure like weak gel, typical for dressing (Bortnowska et al., 2014).

As storage days increased (14 days), dynamic mechanical spectra of USMS did not suffer changes (Fig. 8A and D). Fig. 8B and C showed a relative increased in *G′* modulus after 7 days of storage ($p < 0.05$). Also, the tan *δ* curves of SE1 and SE2 showed an ascending trend at 14 days of storage indicating the evolution of the

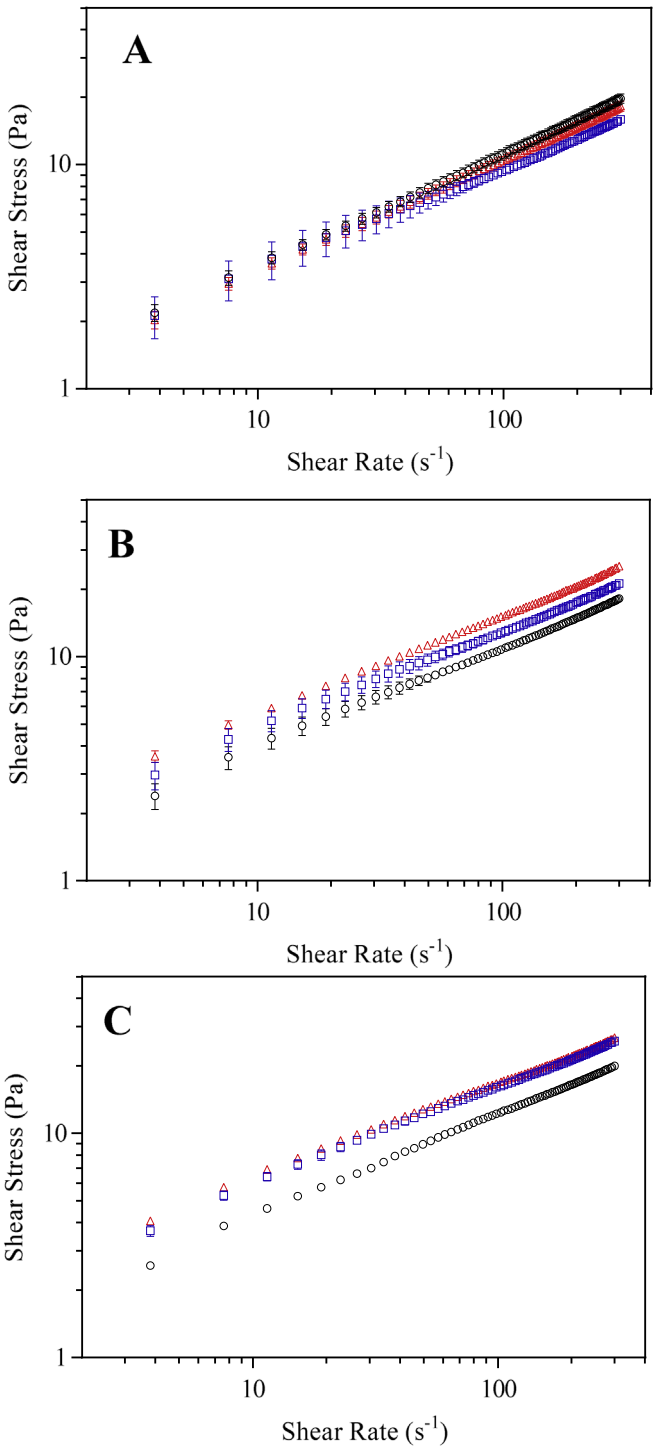

Fig. 7. Flow curves for USMS (A); SE1 (B) and SE2 (C) mixed colloidal suspension during the storage time (days): 0 (◯),7 (□) and 14 (△). Bars represent standard error of the mean (n = 4). Starch suspension (S). Mixed colloidal systems: SE1 (starch suspension - US E1 emulsion) and SE2 (starch suspension – US E2 emulsion).

viscous properties (Fig. 8B and C). Tadros (2004) explained that the values of *G′* increased with increased flocculation, since aggregation of droplets usually result in liquid entrapment and the effective volume fraction of the emulsions shows an apparent increase. This finding would be a real evidence of oil droplet flocculation and its

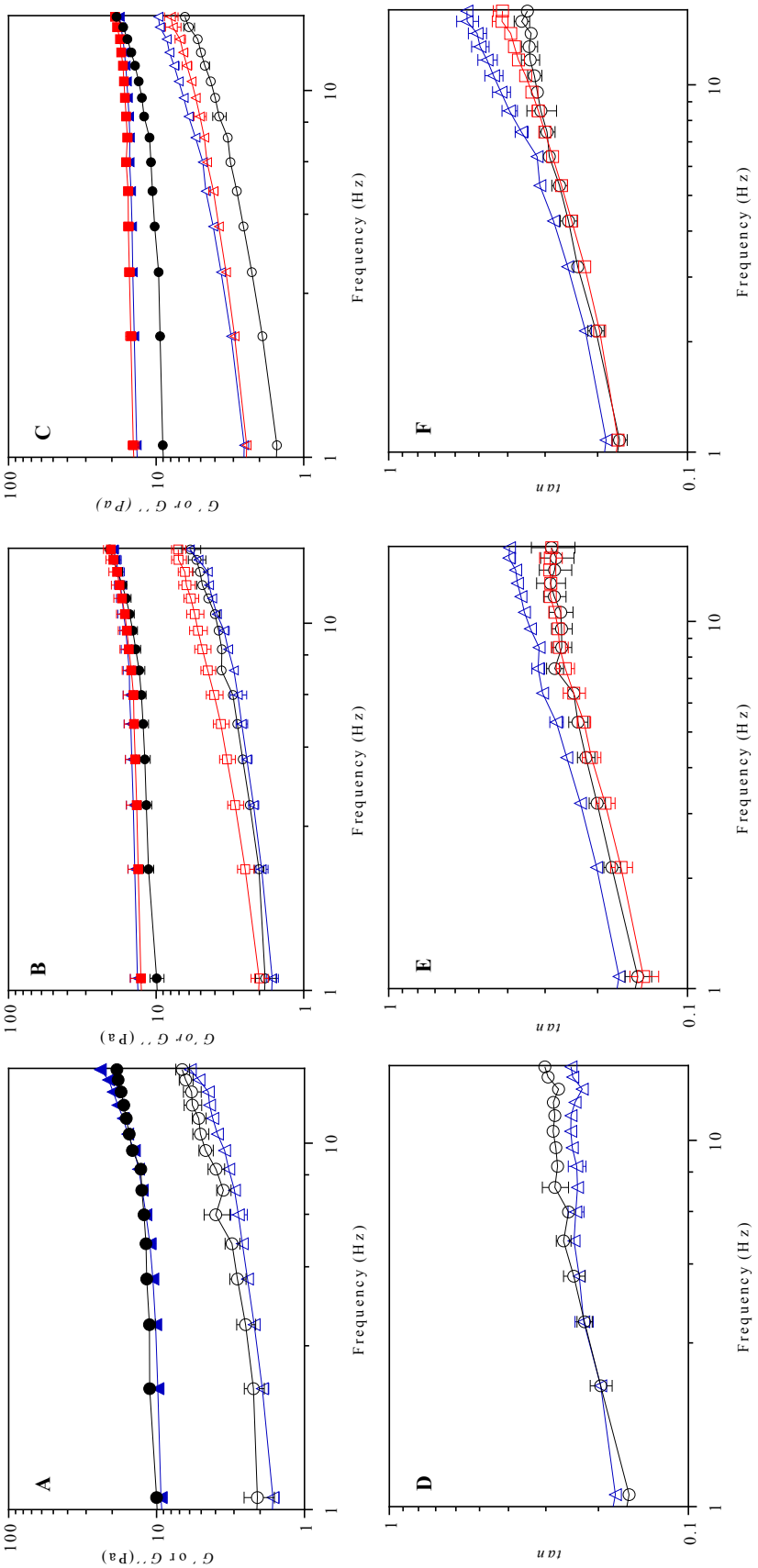

Fig. 8. Effect of storage on mechanical spectra for (A) S; (B) SE1 and (C) SE2 mixed colloidal dispersions during the storage time (days): 0 (●, ○); 7 (■, □) and 14 (▲, △). Solid and empty symbols represent G' and G'', respectively. *Tan* δ of (D) S; (E) SE1 and (F) SE2 during the storage (days): 0 (○), 7 (□) and 14 (△). Mixed colloidal systems: SE1 (starch suspension - US E1 emulsion) and SE2 (starch suspension − US E2 emulsion). Bars represent standard error of the mean (n = 3).

consequence on the viscoelastic properties of each sample. This is in line with previous reports that claimed that flocculation is related to depletion mechanism of destabilization in emulsion after addition of non-absorbing polysaccharides (Chung et al., 2014; Dickinson et al., 1997; Georgiadis et al., 2011).

4. Conclusion

Submicron O/W emulsions prepared with skim milk proteins as emulsifier were prepared and characterized from a rheological, and microstructural point of view. The impact of submicron O/W emulsions incorporation into a modified waxy maize starch based matrix was analysed. These emulsions exhibited Bingham flow type behaviour and the plastic viscosity increased upon 14 days of storage at 5 °C. Flocculation may be responsible for the increase in viscosity with ageing time. Mixed colloidal dispersions (submicron emulsions embedded into starch matrix) showed shear-thinning behaviour. Light microscope micrographs suggested swelling of starch granules with the droplets deposited on the starch granules surface. Flow and viscoelastic behaviour of mixed colloidal dispersions indicated droplets flocculation, attributable to a reversible depletion mechanism of destabilization. These observations have important consequences for encouraging the development of innovative food products.

Acknowledgments

This research was supported by Universidad Nacional de Luján, Universidad de Buenos Aires, Agencia Nacional de Promoción Científica y Tecnológica de la República Argentina (Projects: PICT-2014-1402, PICT-2014-3304 and PICT-2013-1985), Consejo Nacional de Investigaciones Científicas y Tecnológicas (CONICET) and Comisión de Investigaciones Científicas of the Province of Buenos Aires (CIC).

References

Abdolmaleki, K., Mohammadifar, M. A., Mohammadi, R., Fadavi, G., & Meybodi, N. M. (2016). The effect of pH and salt on the stability and physicochemical properties of oil-in-water emulsions prepared with gum tragacanth. *Carbohydrate Polymers, 140*, 342–348.

Aernouts, B., Van Beers, R., Watté, R., Huybrechts, T., Jordens, J., Vermeulen, D., et al. (2015). Effect of ultrasonic homogenization on the Vis/NIR bulk optical properties of milk. *Colloids and Surfaces B Biointerfaces, 126*, 510–519.

Arzeni, C., Martínez, K., Zema, P., Arias, A., Pérez, O. E., & Pilosof, A. M. R. (2012). Comparative study of high intensity ultrasound effects on food proteins functionality. *Journal of Food Engineering, 108*, 463–472.

Bellalta, P., Troncoso, E., Zúñiga, R. N., & Aguilera, J. M. (2012). Rheological and microstructural characterization of WPI-stabilized O/W emulsions exhibiting time-dependent flow behavior. *LWT - Food Science and Technology, 46*, 375–381.

Bortnowska, G., Balejko, J., Tokarczyk, G., Romanowska-Osuch, A., & Krzemińska, N. (2014). Effects of pregelatinized waxy maize starch on the physicochemical properties and stability of model low-fat oil-in-water food emulsions. *Food Hydrocolloids, 36*, 229–237.

Bouyer, E., Mekhloufi, G., Rosilio, V., Grossiord, J.-L., & Agnely, F. (2012). Proteins, polysaccharides, and their complexes used as stabilizers for emulsions: Alternatives to synthetic surfactants in the pharmaceutical field? *International Journal of Pharmaceutics, 436*, 359–378.

Camino, N. A., & Pilosof, A. M. R. (2011). Hydroxypropylmethylcellulose at the oil–water interface. Part II. Submicron-emulsions as affected by pH. *Food Hydrocolloids, 25*, 1051–1062.

Canselier, J. P., Delmas, H., Wilhelm, A. M., Abismail, B., Canselier, H., & Delmas, A. M. (2002). Ultrasound emulsificationdan overview. *Journal of Dispersion Science and Technology, 23*, 333–349.

Chandrapala, J., Martin, G. J. O., Kentish, S. E., & Ashokkumar, M. (2014). Dissolution and reconstitution of casein micelle containing dairy powders by high shear using ultrasonic and physical methods. *Ultrasonics Sonochemistry, 21*, 1658–1665.

Chandrapala, J., Martin, G. J. O., Zisu, B., Kentish, S. E., & Ashokkumar, M. (2012). The effect of ultrasound on casein micelle integrity. *Journal of Dairy Science, 95*, 6882–6890.

Chung, C., Degner, B., & McClements, D. J. (2012). Rheology and microstructure of bimodal particulate dispersions: Model for foods containing fat droplets and starch granules. *Food Research International, 48*, 641–649.

Chung, C., Degner, B., & McClements, D. J. (2014). Understanding multicomponent emulsion-based products: Influence of locust bean gum on fat droplet – starch granule mixtures. *Food Hydrocolloids, 35*, 315–323.

Dickinson, E., Golding, M., & Povey, M. J. W. (1997). Creaming and flocculation of oil-in-water emulsions containing sodium caseinate. *Journal of Colloid and Interface Science, 185*, 515–529.

de Figueiredo Furtado, G., Mantovani, R. A., Consoli, L., Hubinger, M. D., & da Cunha, R. L. (2017). Structural and emulsifying properties of sodium caseinate and lactoferrin influenced by ultrasound process. *Food Hydrocolloids, 63*, 178–188.

Georgiadis, N., Ritzoulis, C., Sioura, G., Kornezou, P., Vasiliadou, C., & Tsioptsias, C. (2011). Contribution of okra extracts to the stability and rheology of oil-in-water emulsions. *Food Hydrocolloids, 25*, 991–999.

Ghosh, V., Mukherjee, A., & Chandrasekaran, N. (2013). Ultrasonic emulsification of food-grade nanoemulsion formulation and evaluation of its bactericidal activity. *Ultrasonics Sonochemistry, 20*, 338–344.

Guo, Z., Zeng, S., Zhang, Y., Lu, X., Tian, Y., & Zheng, B. (2015). The effects of ultra-high pressure on the structural, rheological and retrogradation properties of lotus seed starch. *Food Hydrocolloids, 44*, 285–291.

Kaltsa, O., Spiliopoulou, N., Yanniotis, S., & Mandala, I. (2016). Stability and physical properties of model macro- and nano/submicron emulsions containing fenugreek gum. *Food Hydrocolloids, 61*, 625–632.

Morell, P., Fiszman, S. M., Varela, P., & Hernando, I. (2014). Hydrocolloids for enhancing satiety: Relating oral digestion to rheology, structure and sensory perception. *Food Hydrocolloids, 41*, 343–353.

Nayouf, M., Loisel, C., & Doublier, J. L. (2003). Effect of thermomechanical treatment on the rheological properties of crosslinked waxy corn starch. *Journal of Food Engineering, 59*, 209–219.

O'Sullivan, J., Murray, B., Flynn, C., & Norton, I. (2016). The effect of ultrasound treatment on the structural, physical and emulsifying properties of animal and vegetable proteins. *Food Hydrocolloids, 53*, 141–154.

Robins, M. M., Watson, A. D., & Wilde, P. J. (2002). Emulsions—creaming and rheology. *Current Opinion in Colloid & Interface Science, 7*, 419–425.

Shanmugam, A., & Ashokkumar, M. (2014a). Functional properties of ultrasonically generated flaxseed oil-dairy emulsions. *Ultrasonics Sonochemistry, 21*, 1649–1657.

Shanmugam, A., & Ashokkumar, M. (2014b). Ultrasonic preparation of stable flax seed oil emulsions in dairy systems - physicochemical characterization. *Food Hydrocolloids, 39*, 151–162.

Sosa, N., Schebor, C., & Pérez, O. E. (2014). Encapsulation of citral in formulations containing sucrose or trehalose: Emulsions properties and stability. *Food and Bioproducts Processing, 92*, 266–274.

Tadros, T. (2004). Application of rheology for assessment and prediction of the long-term physical stability of emulsions. *Advances in Colloid and Interface Science, 108–109*, 227–258.

Tárrega, A., Vélez-Ruiz, J. F., & Costell, E. (2005). Influence of milk on the rheological behaviour of cross-linked waxy maize and tapioca starch dispersions. *Food Research International, 38*, 759–768.

Turasan, H., Sahin, S., & Sumnu, G. (2015). Encapsulation of rosemary essential oil. *LWT - Food Science and Technology, 64*, 112–119.

Vu Dang, H., Loisel, C., Desrumaux, A., & Doublier, J. L. (2009). Rheology and microstructure of cross-linked waxy maize starch/whey protein suspensions. *Food Hydrocolloids, 23*, 1678–1686.

Wu, B.-c., & McClements, D. J. (2015). Design of reduced-fat food emulsions: Manipulating microstructure and rheology through controlled aggregation of colloidal particles and biopolymers. *Food Research International, 76*(Part 3), 777–786.